PSCAD/EMTDC-based Simulations for Fault Analysis and Fault Identification in 380V Ring DC Systems

Julia Niewind, Nasser G.A. Hemdan,
Christoph Klosinski, Michael Kurrat
Institute of High Voltage Technology and Electric Power Systems (elenia), Technische Universität Braunschweig
Braunschweig, Germany
n.hemdan@tu-braunschweig.de
c.klosinski@tu-braunschweig.de

Frank Gerdinand[1], Johann Meisner[2] and Stephan Passon[2]
[1]E-T-A Elektrotechnische Apparate GmbH, Altdorf, Germany
[2]Physikalisch-Technische Bundesanstalt (PTB)
Braunschweig, Germany
f.gerdinand@eta.de
johann.meisner@ptb.de
stephan.passon@ptb.de

***Abstract*—With an increasing number of DC driven components in power networks, the introduction of 380V DC distribution grids appears to be a valuable option. Besides all positive aspects of DC systems (e.g. high efficiency, the absence of reactive power, etc.), system protection represents the major challenge which needs to be clarified for DC systems. Advanced AC protection equipment's and methodologies are not sufficient in DC environments. In the current research, fault analysis of 380V DC-Microgrid was performed using PSCAD software. Fault behavior was tested with the application of faults at different locations. All components were connected to the grid through two smart switchgears' which incorporated current and voltage sensors. The recorded data were analyzed and current derivatives were identified as the most crucial parameters for fault detection. Based on that, a credit point concept was set up to filter derivative oscillations in regular operating conditions and to standardize fault indicating values.**

Keywords— DC ring system; fault analysis; fault detection; protection coordination

I. INTRODUCTION

Over the past 100 years, the electrical industry was subjected to massive changes that enable a renaissance of the DC technology today and in the future. An increasing number of today's power sources' and loads' technology is DC driven. This evokes the question of connecting them via DC distribution instead of the commonly used AC grid and hence reducing conversion steps. Moreover, the missing electrical supply for about 1.6 billion people worldwide could be counteracted when providing independent small scale DC Microgrids [1]–[6]. The superiority of DC over AC technology is related to the absence of reactive power demand as well as synchronizing necessities, to higher component efficiency and better power quality as well as reliability. It has been reported for example, that using DC in data centers projects can reduce the energy consumption between 10% to 30% and reducing the capital cost by 15% [7]. All of these incentives will promote introduction of low voltage (i.e. ≤1500 V) DC distribution grids in a valuable option [8]. In the future, the electrical distribution energy grids will not only be operated as AC systems but also as hybrid complex distribution grids. In this context, some parts of the systems will be operated as AC, AC/DC or DC distribution networks. The DC systems are characterized by the existence of a large number of converters, such as load converters, source converters, and power distribution converters [9]. Therefore, the DC systems are converter dominated [10].

In July 2016, Mitsubishi has announced a new lineup (D-SMiree) for low and medium voltage DC systems. The lineup feature products for 380 V DC systems and it is expected to introduce new products for 1500 V DC by 2017 [11]. In December 2012, an IEEE power and energy magazine issue with a title of "plugging into DC" [12] has introduced diverse perspectives for the future distribution grids. The feasibility of using DC technology in households has been discussed in [7]. Many researchers have accomplished a comparison between low voltage AC and DC distribution grids regarding different aspects, such as energy loss, energy efficiency, system stability, and system reliability [8], [13]–[15]. It has been found that the low voltage DC distribution grids can provide an efficient and reliable method of power distribution; new technologies need to be developed in order to make the DC grid real.

In this paper, fault analysis and fault detection in 380V DC ring systems are addressed. Fault detection based on credit point approach (which was proposed by the authors in [16]) will be introduced. Protection in the future DC system represents one of the main challenges, and as the system is built in the ring type, the complexity of fault detection and isolation is increased. In the literature, different fault detection approaches for ring DC systems were developed [17]–[24]. The present work tries to fulfill the gaps in the previously

978-1-5090-4479-5/17/$31.00 ©2017 IEEE

published work as follows:

A. Complexity

Some approaches are complex to be implemented in the real systems (e.g [21], [22]). In [22], the line faults are detected through the measurments at the two ends, and for each line two slaves and one main controllers were assigned. In addition, in [21], a power probe at each point of common connection is needed. In [19], the fault detection is based on H-bridge concept and the power probe unit. In the current work, the proposed method based on modular switches which have been already developed in the lab scale, where the fault detection and isolation depend on simple manipulation of current and voltage measurements on the switchgear itself.

B. Fault detection criteria

In [17], [20], the protection schemes were developed based on the current derivative. The problems associated with the threshold identification for each point in the system prevent this detection concept to be transferred to other topologies. In the current study, the fault detection is conducted based on our proposed scheme [16] which depends on instantaneous switch currents, current derivatives, and credit point of these derivatives, which makes the fault detection more reliable. In [16], the detection approach was implemented on a radial distribution DC system. In the current paper, a new detection algorithm was developed for ring DC systems. The detection algorithm implies cluster and sub-cluster technique.

C. Applicability

The proposed protection technique was developed while practical constraints (e.g. available switchgear, available sampling rate of I/O modules, and available power source technologies, etc.) were taken into consideration. Implementation of the new technique for ring DC system in the lab is planned.

II. System Description

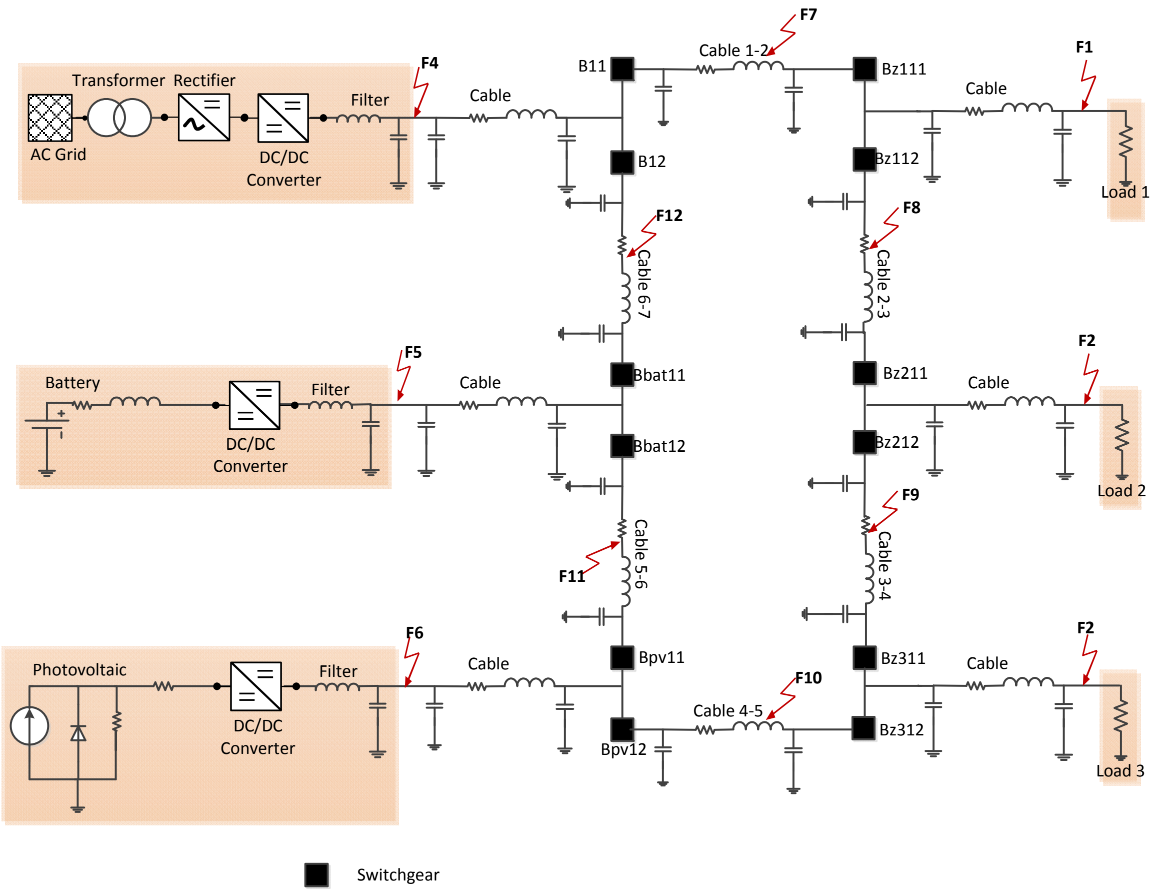

Fig. 1. 380V DC-Microgrid

Figure 1 presents the 380V DC test system which represents a DC ring micro grid. The selected test case can represent a DC-Microgrid. A Microgrid assembles all components of a usual grid, i.e. power generation and loads, on a small space. In addition to the connection to the grid, it also contains storage systems such as batteries. Hence, it can be stand-alone to supply its loads or it can be tied into the overlying network. The Microgrid became only possible due to the introduction of renewable energy sources, which produce electricity at any voltage level depending on the installed capacity. This leads to a change of power flows as today's power generation at low voltage results in bidirectional power flow. A Microgrid structure offers several advantages compared to conventional grid structures. The decentralized power source is closer to the loads and can offer better power quality. Line losses are lower and therefore, the efficiency is better. It guarantees improved reliability as it features redundancies without the need of an expensive meshed grid. As the decentralized energy production is mainly based on renewable energy sources the Microgrid concept also supports the efforts in mitigating climate change as well as electrifying rural areas. Moreover, it may avoid the rising demand in industrial countries to enlarge transmission lines. Despite of such positive factors, there are challenges arising from bidirectional power flow as it features higher system complexity. Therefore, new measuring instruments and control methods need to be researched [25], [26].

The DC-Microgrid topology which has been selected as a case study is given in Fig. 1. The DC-Microgrid is being connected to the 400V AC grid which represents the main power supply. The power flow could generally move either downstream. To operate the conversion from AC to DC or reverse a bidirectional converter is needed. Due to financial reasons for the laboratory equipment's, a unidirectional six pulse rectifier was chosen, i.e. a surplus of energy in the DC system cannot be fed backwards into the AC grid. Boost converters that ensure a stable DC voltage were used to connect the power sources. These converters were designed based on [27].The battery was designed to be able to supply the total load in an islanded mode, while the photovoltaic (PV) was designed to be a supporting entity. The PV system was designed based on the introduced method in [28]. In addition, all sources have been equipped with filters in order to reduce the ripples. All components are separable from the grid through two breakers due to the ring structure. The AC gird, battery, and PV system parameters are given in [16]. The loads as well as the cable parameters are illustrated in Table I.

TABLE I. LOADS AND CABEL PARAMETERS

Loads and Cables			
Load 1	R = 20.37 Ω	Load 3	R = 15.2 Ω
Load 2	R = 10.86 Ω		
Cable Segments	R = 1.07 mΩ/m L = 0.33×10^{-6} H/m	Cable Length	30 m

A. Normal Operation

In normal operation mode, 29.64 kW power as a summation of the three loads are supplied by the three sources. The PV systems supplies 40.1 A, the battery supplies 12.3A and the AC grid supplies 25.3 A.

B. Fault Condition

Two different fault types could occur in the case of ring systems, i.e. parallel and series fault. The parallel fault represents a fault on a component (e.g. load or source) where the series fault represents a fault on a cable or a line. Therefore, in order to isolate the faulty part in case of a parallel as well as a series fault two circuit breakers need to be switched off. Table II illustrates the breaker operation of some parallel and series faults.

TABLE II. BREAKER OPERATION FOR PARALLEL AND SERIES FAULTS IN THE TEST SYSTEM

Breaker	Faults					
	Parallel Faults			*Series Faults*		
	F1	*F2*	*F3*	*F7*	*F8*	*F9*
Bz_{111}	×	-	-	×	-	-
Bz_{112}	×	-	-	-	×	-
Bz_{211}	-	×	-	-	×	-
Bz_{212}	-	×	-	-		×
Bz_{311}	-	-	×	-	-	×
Bz_{312}	-	-	×	-	-	-
B_{11}	-	-	-	×	-	-

As an example the fault currents which are supplied from the AC grid, the battery, and the PV systems are shown in Fig. 2. The total steady state fault current reach 3kA in approximately 44ms. It can be inferred from this figure that the PV system as a current source will supply the same current in normal operation as well as the steady state fault condition. However, the capacitors of the boost converter and the filters which are connecting the PV to the DC-Microgrid will supply a transient fault current. The same concept is valid for the two other sources. As shown in the figure, the battery will supply 84% of the total steady state fault current.

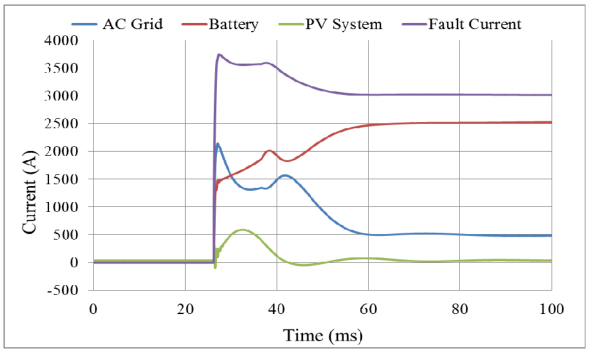

Fig. 2. Power flow in normal operation and fault condition

III. SMS APPROACH

The project Smart Modular Switchgear (SMS) is a research project at Technische Universität Braunschweig for the development of DC protection schemes at different voltage levels. The project aims to providing appropriate algorithms that split the switching task onto several breakers which are located at selected spots in the system. This bears two major advantages: first, a faulted system does not need to get fully de-energized and second; the individual breakers might be much smaller than an overall protective breaker would have to be. The SMS core idea is the smart communication behavior between all system relevant breakers and the switching decision based upon a fault matrix. This matrix is fed by data collected at each circuit breaker which can be called smart and modular according to the explained characteristics [16], [29], [30].

IV. Protection Concept

For the protection of 380 V DC grids, communication between breakers to ensure efficient protection coordination is necessary. The common approach where the AC-system disconnects the whole DC-link in a fault situation leads to a power outage on the DC side. To guarantee reliability in such a system, design of a more advanced solution is desirable. In this paper, a protection concept for 380V DC systems which is developed by the authors in [16] is implemented in order to isolate parallel and series faults in DC-Microgrids.

The protection concept is based on a novel credit point (CP) concept. The proposed approach provides the isolation of only the faulted part while the healthy rest of the system remaining active, trying to keep the disturbance to the lowest possible level. That requires a continuous recording of significant parameters to observe the system status. The protection scheme needs to detect a fault situation and to distinguish it from normal fluctuations. It needs after that to locate it correctly and decide how many and which breakers are needed to be switched off. To achieve that, the diagnosing parameters are assigned to clusters which facilitate the communication within the protection environment. Once the implemented protection coordination identifies a fault according to the input parameters that fed to the background algorithm, the prospected breakers switch off.

The concept is implemented for a ring topology and its robustness is verified by varying of different system specifications. In the ring system given in Fig. 1, all breakers are oriented in the clockwise direction. In the case of a parallel fault, one of the two breakers used for the isolation of each component will always measure large positive values and the other one will measure large negative ones. On the other hand, in normal operation the two breakers on each line segment will always measure the currents in the same direction. And, the current direction will be diverted, in case of a series fault on the line to the fault point and the two breakers will show opposite direction currents.

A. *Approach and Challenges*

Concerning the faults which are depicted in Fig. 1, it has to be noted that initial different fault locations were tested. The decision is taken in favor of the faults that generate the smallest fault currents per branch because they are most difficult to detect. If the algorithm is able to identify those faults correctly it can be assumed that faults with large currents will be detected as well. The farther down the branch a fault is applied, the smaller is the measured fault current at the switchgear. This behavior is foreseeable since cable impedances as well as converters compensate for some of the fault current along the way to the measuring devices. This might explain why all tested faults are located close to the component at the end of each branch.

B. *Fault Detection Concept*

The idea for the developed fault detection concept arises from the initial difficulties with large ripples. As the case study was modeled with a complete model of each component, the ripples in the current and voltages exist. In fault situations, the breakers current derivatives must somehow show a tendency into the same direction as the current itself, the ripples seem to produce a noise that impedes the observation of this tendency. If the noise was reduced, the tendency would become more visible. Implementing the latter running, the recorded derivatives are run through a band stop filter as shown in Fig. 3.

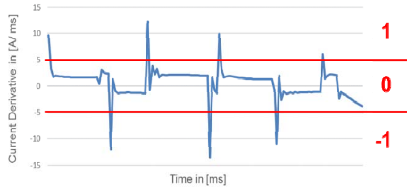

Fig. 3. Model of a band stop filter

The fluctuations around zero is eliminated by rating all records within the band zero, i.e. those above the band 1 and those below the band -1. The output labeled as Credit Points (CP) is then cumulated by a counter with each time step. In steady state condition the sum will always oscillate around zero as only a change in the current magnitude leads to a change in the magnitude of its derivative. If the latter rises above or drops below the filter limits and continues monotonously over several time steps, the counter will show this behavior by also increasing or decreasing, independent of the effective current derivative value. Thus, reaching a value of more than 10 or below -10 clearly indicates a fault state. However, the rated current of the loads needs to be observed simultaneously to avoid an inappropriate switching. Fluctuations in the power consumption may also involve high current derivatives and therefore lead to an increase of counter values. Checking on the compliance with the loads' operating ranges is implemented as an additional requirement. Each fault type develops a specific combination of counter values depending on fault location and component type.

All breakers identify the fault situation simultaneously and the scaling is standardized for all counters. The algorithm which needs to be implemented must be able to identify and locate all possible faults based on their individual combinations of counters to provide the correct output signal of the related breaker(s) to switch off and isolate the faulty part. The general detection procedure is given in [16]. The current magnitude is monitored continuously and a numerical analysis outputs the derivative current values. Those pass a band stop filter which outputs a standardized signal of 1, 0 or -1. A counter attached to each measuring instrument cumulates these credit points and hands the sum over to the protection coordination interface. The latter includes the algorithm that identifies a fault situation according to the counter value combination. It outputs a Boolean signal to the breakers which can be 0 for the unfaulted condition or 1 if the breaker needs to switch off due to a fault incident. The current magnitude itself also feeds the algorithm to allow for larger oscillations within the rated current of loads without identifying them as fault situations.

Subsequently, it is tested if the loads operate outside the normal range. The related breaker only receives a switching signal if both conditions are fulfilled. The simulation time is needed to bridge the transient oscillations which occur when starting the simulation because the detection routine is defined only for the steady state. Resetting the breaker counters is necessary after the isolation of a fault because the CP system only works for an initial state of zero.

C. Fault Detection Algorithm

For the development of the algorithm it is necessary to know which breakers need to be opened in a specific fault situation. For the DC ring topology, each breaker partially protects a component and a line segment as all components operate in parallel and one breaker is installed at each side of the component's connection node. Due to this arrangement, the switching task is always shared by two breakers, either left or right of a connection node to isolate a component's branch or at each end of a line segment to isolate a series fault from the remaining healthy system.

An example of breaker operations subject to the possible faults of the test case is given in Table II. Monitoring of counter values in combination with the provided breaker operation requirements allows allocating the breakers to different clusters which communicate with each other. This offers the advantage that not every single breaker needs to exchange information with all other breakers in the system. The allocation is based on the findings that some breakers show similar behavior in certain fault situations. This knowledge is used to reduce the communication effort and related costs.

Only two clusters are being defined for the studied topology. In future DC systems incorporating a multitude of breakers, the idea of composing clusters which communicate to protect the system instead of having all breakers interact with each other, is expected to increase the overall protection efficiency. In the ring DC topology, the breakers are allocated to clusters referring to series or parallel faults, respectively. The parallel cluster (Cluster 1) consists of each pair breakers used to connect each component (i.e. load or source) to the grid. This cluster is divided into two sub-clusters. The first one represents the loads and the second one represents the sources. The series cluster is divided into sub-clusters, where each sub-cluster represents a line segment in the Microgrid. The fault detection algorithm is shown in Fig. 4.

D. Implementation in PSCAD/EMTDC

The breaker operators provided by PSCAD are based on time input only and cannot be combined to simulate breaker communication which is necessary for the proposed solution. To implement the detection routine a new component is created, whose function is completely programmed by FORTRAN programming language. The input variables for the new component are the individual counter values of each breaker, where CBz1 means credit point (CP) counter values of breaker Bz1.These CP counter values are integer inputs. The measured current is provided as input in addition to the simulation time. These two input categories are real values. A logical signal for each breaker is the main output of the component. Another logical signal is a parameter called rest breaker. It can only transmit a Boolean 1 or a 0 and is used to reset the counters at the breakers to zero after they have exceeded the threshold due to a fault incident. The simulation is being processed with a time step of 5 μs and 20 μs over a simulation time of 1 second.

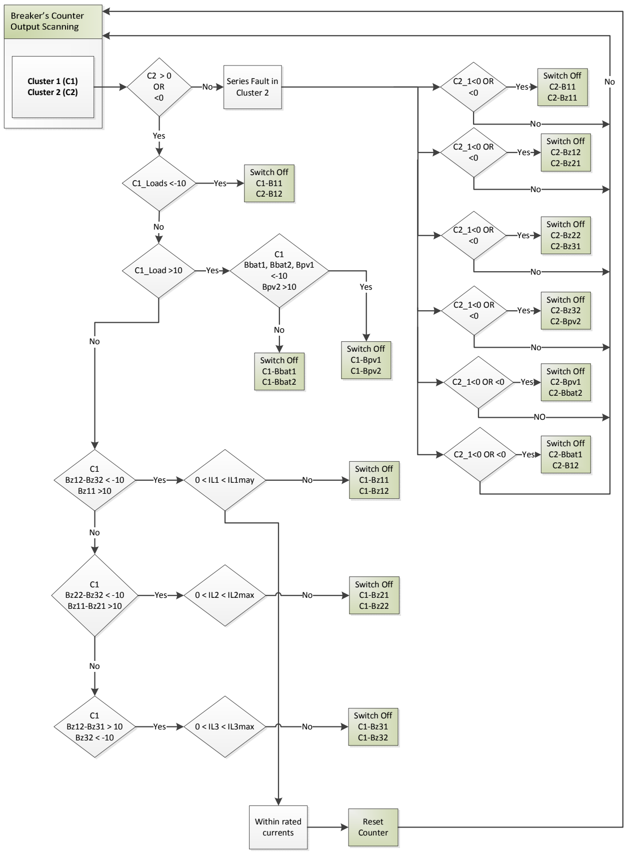

Fig. 4. Fault detection and allocation algorithm

V. RESULTS AND DISCUSSION

At first sight, the fault detection appears more difficult in ring topologies than in radial ones. The counters will be activated as long as the derivatives surpass the band stop filter limits. One advantage of the ring topology compared to the radial topology is the higher reliability. There is no fault situation that would lead to a power outage for the ring structure. A fault may appear on the line or at a component and both cases can be reliably switched off without interrupting the power supply of the remaining healthy system. A fault at a load is illustrated in Fig. 5 as an example of fault F1. It reveals the characteristic behavior of parallel faults in a ring topology.

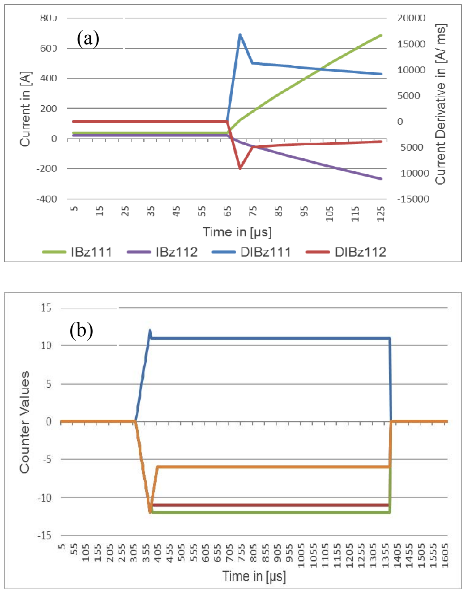

Fig. 5. Fault F1 (a) Currents and current derivatives (b) Counter outputs (Loads breakers)

Figure 5 shows that the currents at the two breakers, which are installed left and right of the connection node, drift in opposite directions. Their derivatives behave accordingly. The fault which is initiated at the branch of a load is fed from both sides of the ring. The PV plant mainly supplies fault current via the lower part of the ring and the AC grid feeds the fault via the upper part of the ring.

As all breakers are installed with the same orientation (clockwise), one of the load breakers records negative values and the other one records positive current flow. The rising difference between the measured currents at the two switchgears adds up to the total fault current. Faults which are applied at one of the sources show smaller surge currents through each breaker in the ring structure than in the data center topology. Based on derivative values a change of the system behavior can be identified earlier than with only observing the currents. Thus, the CP concept also reacts to faults with slowly rising fault currents. Figures 6 and 7 show the development of currents and their derivatives in a faults F4 (AC grid) and F6 (PV system). It can be inferred from these figures that in such fault cases the detection can be proceed within less than 100 µs. In contrast to the above discussed sources' fault detection, the isolation of a fault at the battery takes comparably long time; this can be seen in Fig. 8. The recorded values show the situation in the instant before the switching operation. The detection time of approximately 1ms, this circumstance is rather caused by the arrangement of components in a ring topology. The battery is located between the PV plant and the AC supply. Due to the ring structure, the power supplied by the battery passes the other sources first before proceeding to the loads.

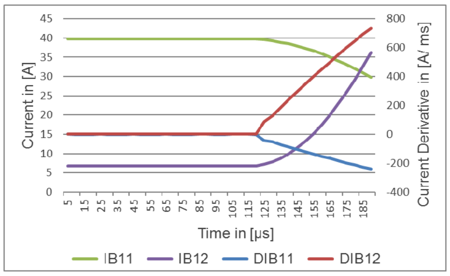

Fig. 6. Currents and current derivatives (for breakers B11, B12) in case of fault F4

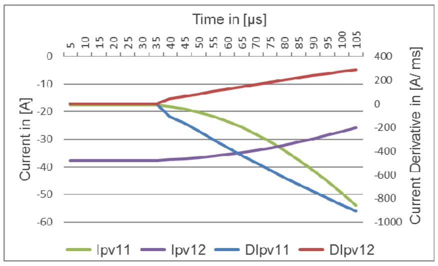

Fig. 7. Currents and current derivatives (for breakers Bpv11, Bpv12) in case of fault F6

According to Fig. 9 the counters of the sources react instantaneously at fault initiation, whereas the loads counter in Fig. (b) start adding credit point in a later moment. High fault currents measured at the battery breakers are the main consequences of such late isolation. Besides parallel faults, the ring topology also bears series fault situations which occur when a cable is faulty. These faults are easy to be identified as they constitute the only case in which the currents at the two line breakers have diverging directions. No other situation would lead to such characteristic. Therefore, their detection time can be kept short and the current direction is the only parameter observed. As soon as the current derivatives and the counters of two series breakers drift away from each other, the activating signal is sent and the breakers immediately switch off. Figure 10 illustrates this fault situation F8. Only 10 µs pass until the fault is identified and located.

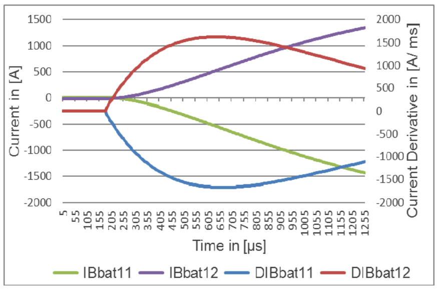

Fig. 8. Currents and current derivatives (for brealers Bbat11, Bbat12) in case of fault F5

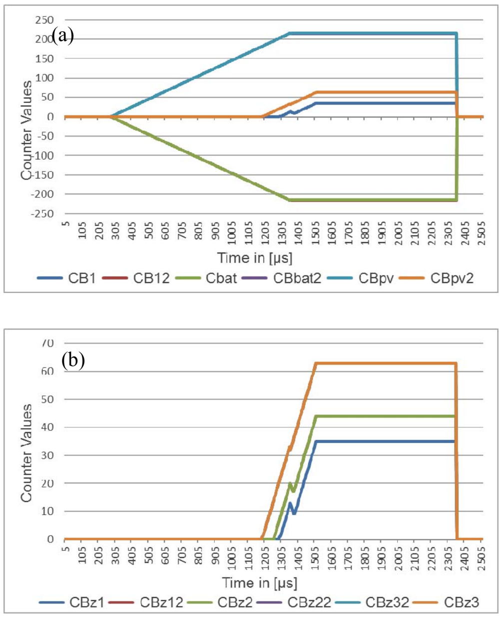

Fig. 9. Counter outputs in case of fault F5 (a) Sources (b) Loads

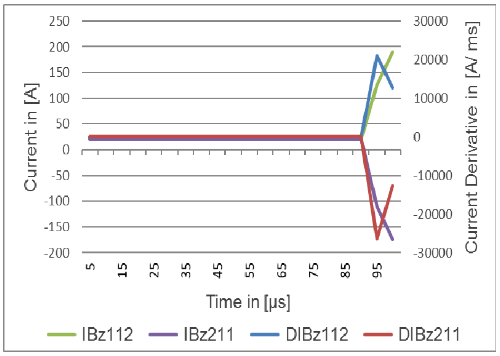

Fig. 10. Fault F8, currents and current derivatives through the two breakers connecting the line

Table III summarizes the detection times for some faults. The fault isolation occurs one time step ahead of the detection time because the simulated breakers are assumed to be ideal. Adding 5 µs to the presented values results in the time period between application of fault and switching off the relevant breakers.

TABLE III. DETECTION TIME FOR DIFFERENT FAULT LOCATIONS

Fault	Detection Time [µs]
F1	55
F2	55
F3	55
F4	65
F5	1070
F6	70
F7	10

VI. CONCLUSIONS

The developed protection concept assigns credit points (CPs) according to the current derivative values. This scheme successfully detects fault cases with detection periods ranging between 0.06 ms and 1.07ms. Each fault applied to the systems leads to the correct signal which activates the equivalent circuit breaker. The fault detection algorithm is robust as changes of resistances, e.g. for the loads, faults or the earthing, or of cable length have no influence on their detection capability. This highlights their accurate selectivity. Moreover, faults can be clearly distinguished from random variations which occur due to variation in the loads' operating ranges. These may also evoke steep slopes of current derivatives. The algorithm recognizes such events for two reasons. Firstly, the mentioned spikes might last for only few time steps and then fall between the limits of the band stop filter so that no further CPs are triggered. Regardless to a fault case or non-fault case, the counters are reset to zero with the implemented time delay when exceeding the defined thresholds. The algorithm requires small adaptations when applied with a solution time step of 20 µs instead of 5 µs. For the second topology, adaptations are only necessary for the detection of a faulty battery. It can be said that the battery in the ring topology poses problems with both time steps, which need to be addressed in future work.

ACKNOWLEDGMENT

The authors would like to thank the German Federal Ministry of Education and Research for the financial support.

REFERENCES

[1] J. Niewind, "Protection Coordination in 380 V DC Grids," Technische Universität Braunschweig, 2016.

[2] M. März, "Niederspannungs-Gleichstromnetze," in Cluster-Semiar LV -DC-Grids, 2012, pp. 1–31.

[3] B. Wunder, "380V DC in Commercial Buildings and Offices," in VICOR seminar 2014, Fraunhofer Institute of Integrated Systems and Device Technology, 2014, p. 71.

[4] D. Symanski and G. Stuebing, "DC Distribution in Data Centers and Telecom Central Offices," 2012.

[5] Taufik, "The DC House Project: Providing access to electricity for the less fortunates," 2010. [Online]. Available: http://www.calpoly.edu/~taufik/dchouse/.

[6] B. Nordman and K. Christensen, "DC Local Power Distribution: Technology, Deployment, and Pathways to Success," IEEE Electrif. Mag., vol. 4, no. 2, pp. 29–36, 2016.

[7] A. Shivakumar, B. Normark, and M. Welsch, "Household DC networks : State of the art and future prospects," Rapid Response Energy Br., no. September, 2015.

[8] A. T. Elsayed, A. A. Mohamed, and O. A. Mohammed, "DC microgrids and distribution systems: An overview," Electr. Power Syst. Res., vol. 119, pp. 407–417, 2015.

[9] D. Boroyevich, I. Cvetković, D. Dong, R. Burgos, F. Wang, and F. Lee, "Future electronic power distribution systems - A contemplative view," in Proceedings of the International Conference on Optimisation of Electrical and Electronic Equipment, OPTIM, , pp. 1369–1380,2010.

[10] A. A. A. Radwan, Y. A. R. I. Mohamed, and E. F. El-Saadany, "Assessment and performance evaluation of DC-side interactions of voltage-source inverters interfacing renewable energy systems," Sustain. Energy, Grids Networks, vol. 1, pp. 28–44, 2015.

[11] M. Electric, "Mitsubishi Electric Launches D-SMiree System for Medium- and Low-voltage DC Distribution," MITSUBISHI Electr.,

pp. 1–4, 2016.
[12] "Plugging into DC, Edison would be happy," IEEE Power&Energy Mag., vol. 10, no. 6, 2012.
[13] M. Amin, Y. Arafat, S. Lundberg, and S. Mangold, "Low voltage DC distribution system compared with 230 V AC," 2011 IEEE Electr. Power Energy Conf., pp. 340–345, Oct. 2011.
[14] D. Hammerstrom, "AC Versus DC Distribution Systems Did We Get it Right?," in Power Engineering Society General Meeting, IEEE, pp. 1–5, 2007.
[15] T. Kaipia, P. Salonen, J. Lassila, and J. Partanen, "Possibilities of the low voltage dc distribution systems," pp. 1–10.
[16] J. Niewind, N. G. A. Hemdan, C. Klosinski, D. Bösche, M. Kurrat, F. Gerdinand, J. Meisner, and S. Passon, "Operation and Protection of 380V DC Distribution Systems," in PowerTech2017, 2017.
[17] M. Farhadi and O. A. Mohammed, "A New Protection Scheme for Multi-Bus DC Power Systems Using an Event Classification Approach," IEEE Trans. Ind. Appl., vol. 52, no. 4, pp. 2834–2842, 2016.
[18] A. J and P Kanakasabapathy, "Protection of a Low-Voltage DC Ring Microgrid System," in International Conference onEnergy Efficient Technologies for Sustainability (ICEETS), 2016, pp. 17–22.
[19] R. Kheirollahi and E. Dehghanpour, "Developing a New Fault Location Topology for DC Microgrid Systems," in 7th Power Electronics, Drive Systems & Technologies Conference (PEDSTC 2016), 2016, no. Pedstc, pp. 16–18.
[20] A. Meghwani, S. C. Srivastava, and S. Chakrabarti, "A new protection scheme for DC microgrid using line current derivative," in IEEE Power and Energy Society General Meeting, 2015, vol. 2015–Septe, pp. 1–5.
[21] J. Do Park, J. Candelaria, L. Ma, and K. Dunn, "DC ring-bus microgrid fault protection and identification of fault location," IEEE Trans. Power Deliv., vol. 28, no. 4, pp. 2574–2584, 2013.
[22] J. Park and J. Candelaria, "Fault Detection and Isolation in Low-Voltage DC-Bus Microgrid System," IEEE Trans. Power Deliv., vol. 28, no. 2, pp. 779–787, 2013.
[23] L. Tang and B. T. Ooi, "Locating and isolating DC faults in multi-terminal DC systems," IEEE Trans. Power Deliv., vol. 22, no. 3, pp. 1877–1884, 2007.
[24] M. Yu, Y. Wang, L. Zhang, and Ziguang Zhang, "DC Short Circuit Fault Analysis and Protection of Ring Type DC Microgrid," in IEEE 8th International Power Electronics and Motion Control Conference (IPEMC-ECCE Asia) DC, 2016, pp. 1–7.
[25] J. J. Justo, F. Mwasilu, J. Lee, and J. W. Jung, "AC-Microgrids versus DC-Microgrids with Distributed Energy Resources: A Review," Renew. Sustain. Energy Rev., vol. 24, no. August, pp. 387–405, 2013.
[26] F. Blaabjerg and J. M. Guerrero, "Smart Grid and Renewable Energy Systems," in International Conference onElectrical Machines and Systems (ICEMS), 2011, pp. 1–10.
[27] R. Shaffer, Fundamentals of Power Electronics with MATLAB. Boston, Massachusetts: Charles River Media, 2007.
[28] M. G. Villalva, J. R. Gazoli, and E. F. Ruppert, "Modeling and Circuit-Based Simulation of Photovoltaic Arrays," Brazilian J. Power Electron., vol. 14, no. 1, 2009.
[29] C. Klosinski, N. G. A. Hemdan, M. Hilbert, P. M. Kurrat, F. Gerdinand, E. E. A. Gmbh, and K. Von Gleichspannungsnetzen, "Smart Modular Switchgear für den Einsatz in Gleichstromsystemen," in Albert-Keil-Kontaktsemina, AKK, 2015.
[30] N. G. A. Hemdan, C. Klosinski, M. Hilbert, M. Kurrat, F. Gerdinand, J. Meisner, and Stephan Passon, "Fault Matrix Based Protection Coordination in Low Voltage DC Systems," in International Conference on Power Systems Technology, 2016, pp. 1–6.